Small-Scale Dynamics of High–Reynolds-Number Two-Dimensional Turbulence

M. E. Brachet,[1] M. Meneguzzi,[2] and P. L. Sulem[1,3]

[1]*Centre National de la Recherche Scientifique, Observatoire de Nice, 06003 Nice, France*

[2]*Service d'Astrophysique, Centre D'Etudes Nucléaires de Saclay, 91191 Gif-sur-Yvette, France, and Centre National de la Recherche Scientifique, Gif-sur-Yvette, France*

[3]*School of Mathematical Sciences, Tel Aviv University, Tel Aviv, Israel*

(Received 12 August 1985)

The free decay of two-dimensional turbulence is simulated by direct numerical integration of the incompressible Navier-Stokes equations at resolutions 512^2 and, for flows with symmetries, 1024^2. At early times, quasirectilinear vorticity-gradient sheets develop, with a thickness decaying exponentially in time until dissipation becomes relevant. The energy spectrum then displays a k^n range with $n \simeq -4$. At later times, we observe a transition to $n \simeq -3$. Vorticity gradients are then distributed on reconnecting, elongated, dissipative structures.

PACS numbers: 47.25.–c, 61.20.Ja

A controversial question concerning high–Reynolds-number turbulence in two-dimensional incompressible flows is the behavior of the small-scale energy spectrum. Saffman[1] argues that advection will bring different values of vorticity close together, producing thin sheets of vorticity gradient and leading to a k^{-4} inertial energy spectrum. In contrast, the statistical theory of the enstrophy cascade of Kraichnan[2] and Batchelor[3] predicts a k^{-3} energy spectrum, with a possible logarithmic correction due to nonlocal interactions.[4] Furthermore, Kraichnan[5] argues that because of this nonlocality, intermittency will not affect the small-scale energy spectrum.

Since the first calculations of Lilly,[6] it has been recognized that high resolutions are required to simulate an inertial range properly.[7] Preliminary computations at 512^2 resolution presented by Orszag[8] showed that when the large-scale Reynolds number is increased from 1100 to 25 000, a distince change is observed from a k^{-4} energy spectrum to a spectrum roughly proportional to k^{-3}. Calculations at a similar resolution have recently been done by Satofuka, Nakamura, and Nishida.[9]

In this Letter, we present new results on small-scale dynamics obtained by direct numerical simulations. This includes the time evolution of the spectral exponent n which displays a transition from an early $n \simeq -4$ to $n \simeq -3$ corresponding to a more mature flow. Visualizations in physical space are also presented. We report here on two computations. The first one was done with general periodic boundary conditions at 512^2 resolution (on a CRAY-XMP with 2 megawords of memory). The other was done with a flow presenting large-scale symmetries analogous to those of the (three-dimensional) Taylor-Green vortex.[10] These symmetries enabled us to use a resolution of 1024^2 on a CRAY-1S with 1 megaword memory. Calculations at higher resolution are under way and will be reported in a more extended paper.

(1) *General periodic flow.*—The initial velocity field is a zero-mean Gaussian random function with an energy spectrum

$$E(k,0) = C_0 k e^{-(k/k_0)^2}. \tag{1}$$

We choose $k_0 = 2$, $C_0 = 0.02$, and a viscosity $\nu = 1.5 \times 10^{-4}$.[11] In our realization, the energy is $\Sigma = 0.06$ and the enstrophy $\Omega = 0.34$. A pseudospectral method based on Fourier-mode expansion is used for space variables. Time marching is done with a stabilized leapfrog-Crank-Nicholson scheme.

The short-time behavior of the flow is observed to be dominated by the formation of vorticity-gradient sheets. A simple modeling of this phenomenon is obtained from the inviscid equation for the curl of vorticity:

$$(\partial_t + \mathbf{v}\cdot\nabla)\nabla\times\boldsymbol{\omega} = \nabla\times\boldsymbol{\omega}\cdot\nabla\mathbf{v}. \tag{2}$$

If, following Weiss,[12] we assume scale separation between $\nabla\times\boldsymbol{\omega}$ and a much more slowly varying $\nabla\mathbf{v}$, then Eq. (2) is essentially linear in Lagrangean coordinates and leads either to an exponential growth of $\nabla\times\boldsymbol{\omega}$ if strain dominates vorticity, or to an oscillatory behavior if rotation dominates. In the former case, $\nabla\times\boldsymbol{\omega}$ is locally elongated along one eigendirection and contracted along the other.

During this period of vorticity-gradient sheet formation, the exponential tail of the energy spectrum has a logarithmic decrement β decaying exponentially in time. This behavior, which reflects the presence of complex singularities approaching the real domain,[13] could probably be described by a model of sheet formation analogous to that given in the appendix of Ref. 10. This exponential flattening is stopped when dissipation becomes relevant (with our conditions, when $\beta \simeq 0.1$). In Fourier space, we then observe a k^n range in the energy spectrum, with a spectral index

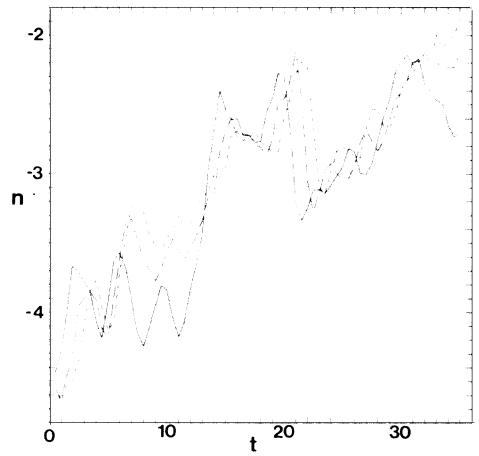

FIG. 1. Spectral index n vs time for general periodic flow, obtained by fitting of the energy spectrum with $E(k) = Ck^n \exp(-\beta k)$ in the ranges: $5 < k < 40$ (solid line), $5 < k < 60$ (dashed line), $5 < k < 80$ (dotted line).

fluctuating around the value $n \simeq -4$ predicted by Saffman.[1] At scales large compared to the sheet thickness, these can indeed be viewed as quasidiscontinuities of vorticity. The value of n is determined by a least-squares fit of the energy spectrum with a function of the form $E(k) = Ck^n \exp(-\beta k)$ (Fig. 1) as well as by direct inspection of the spectrum [Fig. 2(a)]. In Fig. 1, the best fit is represented by the solid line and corresponds to $5 < k < 40$. The two other fits are obtained on ranges which are sensibly more extended than the inertial range seen in Fig. 2. They are thus more affected by the algebraic prefactor of the dissipation range. These curves nevertheless give an estimate of the sensitivity of the results to the fit interval.

The k^{-4} energy spectrum is only visible during a short period of time. When the flow becomes more mature (namely, a few turnover times before the enstrophy dissipation reaches its maximum), the spectral index increases sharply to values close to -3 [Figs. 1 and 2(b)]. In physical space, elongated vorticity-gradient sheets resulting from squeezing of vorticity blobs are visible. They first tend to become aligned in a fixed direction and to pile up (Fig. 3). Dissipation and straining then act to restore a simpler structure. The process is reproduced as other vorticity sheets approach the active region. A simple model of this process is obtained by our considering vorticity as a passive scalar subject to external injection, straining, and dissipation. Transposition of the Batchelor passive scalar analysis[14-16] leads to a k^{-3} energy inertial range, but also to a pathological (nonexponential) dissipative range (except for very special statistics of the large-scale straining[5]). This suggests that nonlinear effects have to be taken into account to describe correctly the dissipation range and also, as noted in Ref. 5, to obtain logarithmic corrections to the k^{-3} inertial range.

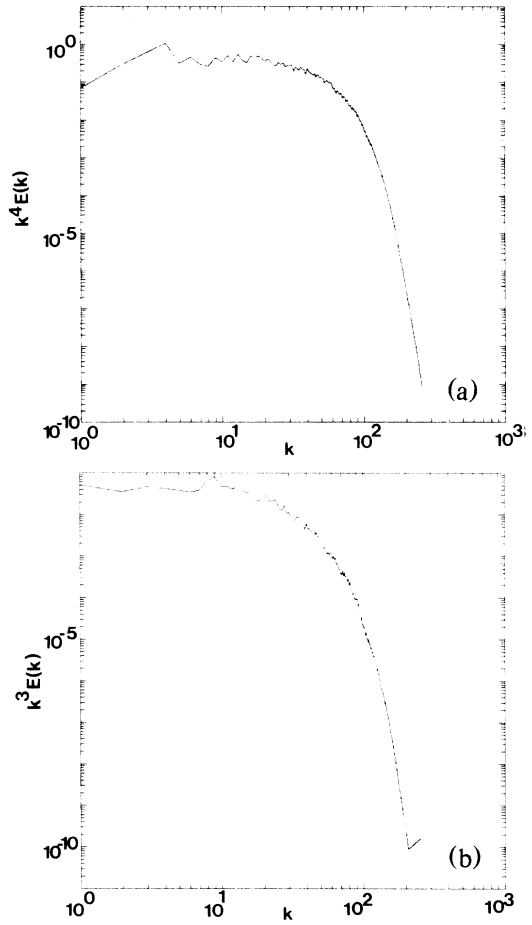

FIG. 2. (a) $k^4E(k)$ vs k at $t = 10$; (b) $k^3E(k)$ vs k at $t = 29$ (same run as Fig. 1).

(2) *Symmetric flows.*—We briefly discuss in this section the case of (initially Gaussian) random flows with large-scale symmetries, analogous to those of the (three-dimensional) Taylor-Green vortex.[10] The stream function is assumed to have the Fourier representation

$$\psi(x,y,t) = \sum_{l,m=0}^{N/2} a_{lm}(t) \sin lx \sin my, \tag{3}$$

where the coefficients a_{lm} vanish unless l and m are both even or both odd integers. This representation is compatible with Navier-Stokes dynamics and corresponds in physical space to the following flow symmetries: (i) invariance by rotation of π around the point $x = \pi/2$, $y = \pi/2$; (ii) reflectional symmetries on the sides of an impermeable box given by $x = 0$ and π, $y = 0$ and π.

Two computations with the same initial conditions are presented. The initial energy spectrum is given by Eq. (1), with $k_0 = 5$ and $C_0 = 0.02$. For our particular realization the energy is 0.61 and the enstrophy 3.6. The viscosity is $\nu = 0.7 \times 10^{-4}$ and 2.35×10^{-5}, respec-

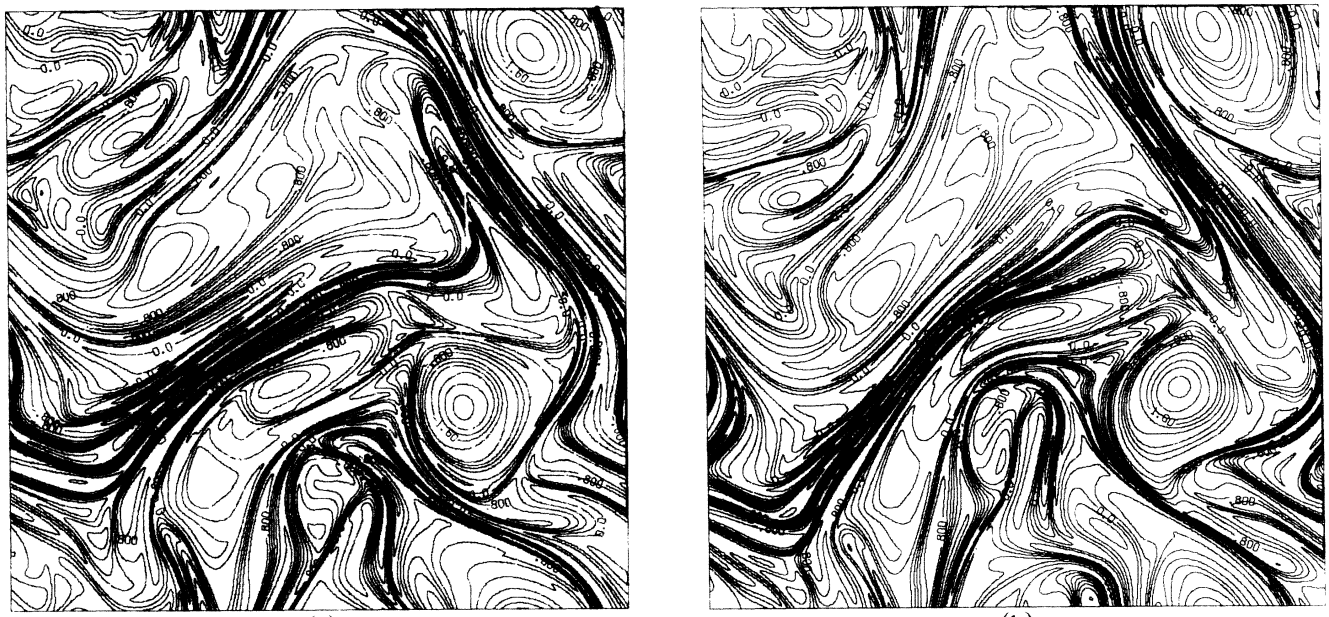

(a) (b)

FIG. 3. Isovorticity lines for general periodic flow (same run as Figs. 1 and 2) at (a) $t = 20$ and (b) $t = 22$.

tively. Results concerning symmetric two-dimensional flows were previously reported.[17-19] The main observation is the qualitative similarity of the small-scale dynamics of flows with and without large-scale symmetries. It is again dominated by the formation of elongated vorticity-gradient sheets, which may eventually merge (Fig. 4), and in Fourier space by the transition from a k^{-4} to a k^{-3} energy inertial range (Fig. 5). Here, the k^{-4} period is much shorter than in the nonsymmetric runs. The reason is that we are using initial conditions with a smaller integral scale and comparable energy. As a consequence, all the dynamics is accelerated. Note, however, that the impermeable box produces a bending of the vorticity-gradient sheets.

In none of our runs do we observe the emergence of coherent persistent isotropic vortices analogous to those observed by McWilliams.[20] This is probably a

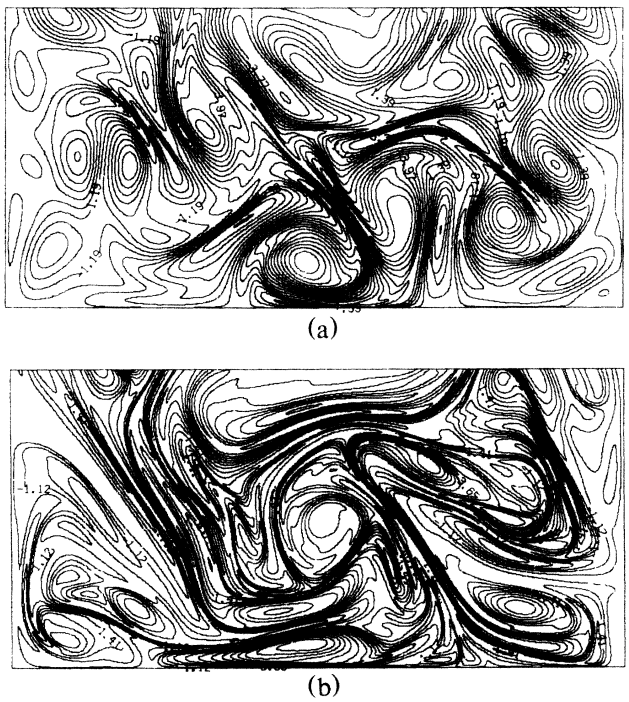

(a) (b)

FIG. 4. Isovorticity lines for the symmetric flow with $\nu = 7 \times 10^{-5}$ at (a) $t = 1$ and (b) $t = 2$ in the domain $0 \leq x \leq \pi$, $0 \leq y \leq \pi/2$.

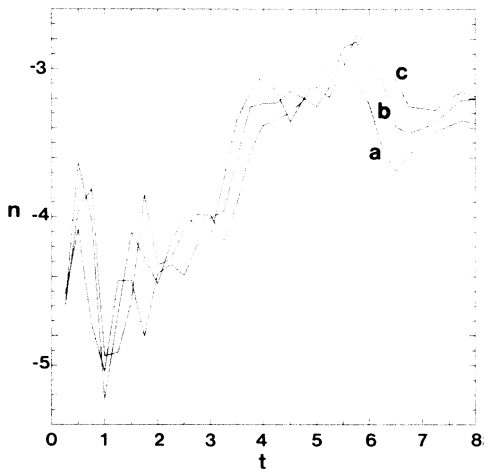

FIG. 5. Spectral index n vs time for the symmetric flow with $\nu = 2.35 \times 10^{-5}$. The three curves correspond to fits in the ranges (curve a) $10 < k < 170$, (curve b) $10 < k < 256$, and (curve c) $10 < k < 340$.

consequence of the much smaller integral scale (compared to the spatial period) and/or the very long integration time (compared to the time of maximum enstrophy dissipation) of his calculation.

We thank U. Frisch, J. Herring, R. H. Kraichnan, S. A. Orszag, and J. C. McWilliams for very useful discussions and suggestions. We also thank H. Politano, who made flow visualizations on the VICOM of the Nice Observatory Direction des Recherches, Etudes et Techniques Contract No. 82/522). The computations were done on the Cray 1S of the Centre de Calcul Vectorielle pour la Recherche, Ecole Polytechnique (Palaiseau) and on the Cray-XMP of Compagnie Internationale de Services en Informatique Computer Center of Saclay using fast Fourier transforms of C. Temperton and S. A. Orszag and the National Center for Atmospheric Research graphics software.

[1]R. G. Saffman, Stud. Appl. Math. **50**, 377 (1971).
[2]H. R. Kraichnan, Phys. Fluids **10**, 1417 (1967).
[3]G. K. Batchelor, Phys. Fluids **12**, 233 (1969).
[4]H. R. Kraichnan, J. Fluid Mech. **47**, 525 (1971).
[5]H. R. Kraichnan, J. Fluid Mech. **67**, 155 (1975).
[6]D. K. Lilly, Phys. Fluids, Suppl. **12**, 240 (1969).
[7]J. R. Herring, S. A. Orszag, H. R. Kraichnan, and D. G. Fox, J. Fluid Mech. **66**, 417 (1974).
[8]S. A. Orszag, in *Proceedings of the Fifth International Conference on Numerical Methods in Fluid Dynamics,* edited by A. I. van de Vooren and P. J. Zandbergen, Lecture Notes in Physics Vol. 59 (Springer, Berlin, 1977), p. 32.
[9]N. Satofuka, H. Nakamura, and H. Nishida, in *Ninth International Conference on Numerical Methods in Fluid Dynamics,* edited by J. P. Boujot, Lecture Notes in Physics Vol. 218 (Springer, Berlin, 1984), p. 475.
[10]M. E. Brachet, D. I. Meiron, S. A. Orszag, B. G. Nickel, R. H. Morf, and U. Frisch, J. Fluid Mech. **130**, 411 (1983).
[11]This choice of parameters corresponds to the highest Reynolds number achievable at 512^2 resolution while still resolving precisely the smallest scales.
[12]J. Weiss, La Jolla Institute Report No. LJI-TN-81-121, 1981 (unpublished).
[13]C. Sulem, P. L. Sulem, and H. Frisch, J. Comput. Phys. **50**, 138 (1983).
[14]G. K. Batchelor, J. Fluid Mech. **5**, 113 (1959).
[15]H. R. Kraichnan, Phys. Fluids **11**, 945 (1968).
[16]D. C. Leslie, *Developments in the Theory of Turbulence* (Clarendon, Oxford, 1973).
[17]M. E. Brachet and P. L. Sulem, in Proceedings of the Fourth Beer Sheva Seminar on MHD Flows and Turbulence, Prog. Astronaut. Aeronaut. (to be published).
[18]M. E. Brachet and P. L. Sulem, in Ref. 9, p. 103.
[19]M. E. Brachet, M. Meneguzzi, and P. L. Sulem, in *Macroscopic Modeling of Turbulent Flows,* edited by U. Frisch *et al.,* Lecture Notes in Physics Vol. 230 (Springer, Berlin, 1985), p. 347.
[20]J. C. McWilliams, J. Fluid Mech. **146**, 21 (1984).

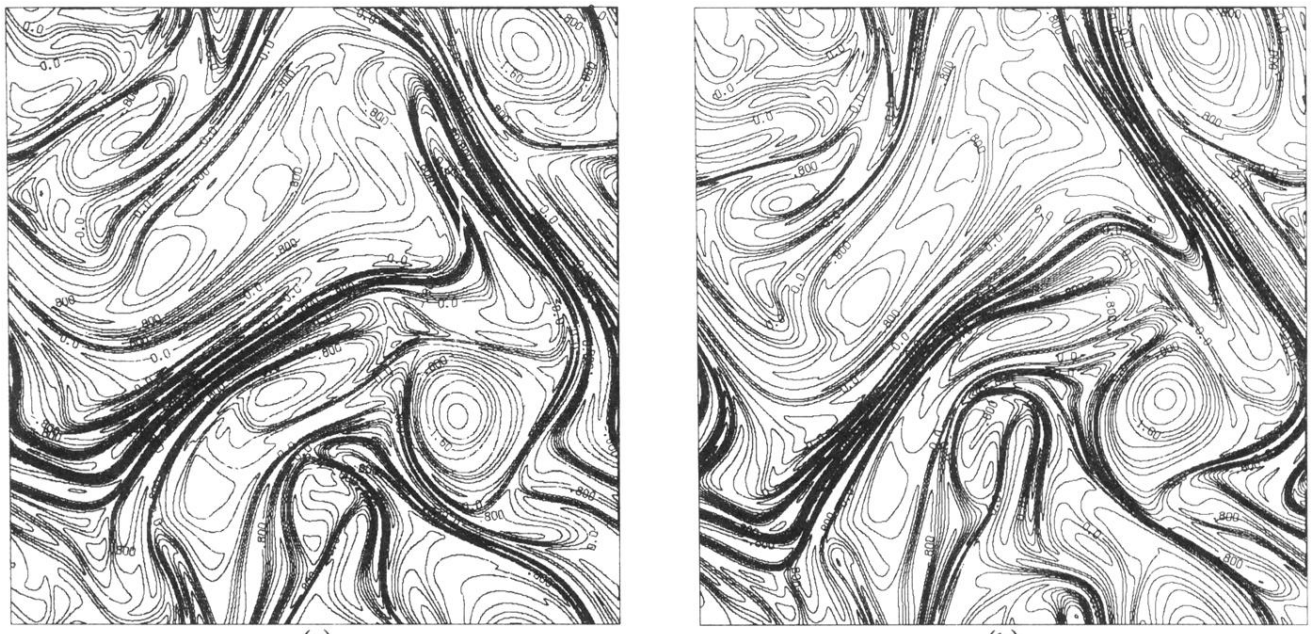

(a) (b)

FIG. 3. Isovorticity lines for general periodic flow (same run as Figs. 1 and 2) at (a) $t = 20$ and (b) $t = 22$.

(a)

(b)

FIG. 4. Isovorticity lines for the symmetric flow with $\nu = 7\times 10^{-5}$ at (a) $t=1$ and (b) $t=2$ in the domain $0 \leq x \leq \pi$, $0 \leq y \leq \pi/2$.